agriculture

MDPI

Article

Design and Experiment of Obstacle Avoidance Mower in Orchard

Yi Yang [1,2], Yichuan He [2,3,4,5,*], Zhihui Tang [2,3,6] and Hong Zhang [2,3,6]

[1] Xingxin Vocational and Technical College of Xinjiang Production and Construction Corps, Tiemenguan 841007, China; 10757222236@stumail.taru.edu.cn
[2] Xinjiang Production and Construction Corps (XPCC) Key Laboratory of Utilization and Equipment of Special Agricultural and Forestry Products in Southern Xinjiang, Tarim University, Alar 843300, China; 120230164@taru.edu.cn (Z.T.); 120050025@taru.edu.cn (H.Z.)
[3] College of Mechanical and Electronic Engineering, Tarim University, Alar 843300, China
[4] College of Technology, Huazhong Agricultural University, Wuhan 430070, China
[5] School of Mechanical Science and Engineering, Huazhong University of Science and Technology, Wuhan 430074, China
[6] Key Laboratory of Tarim Oasis Agriculture Ministry of Education, Tarim University, Alar 843300, China
* Correspondence: heyc@taru.edu.cn

Abstract: In order to solve the problem of mowing between plants in Xinjiang trunk orchards, an obstacle avoidance mower suitable for trunk orchard planting mode was designed. The whole structure, working principle and main parameter design of the obstacle avoidance mower are introduced. The finite element analysis and kinematic analysis of the cutter are carried out on the premise of using a Y-shaped cutter and its arrangement, and the condition that the inter-row mower does not leak is determined. Through the modal analysis of the frame, the range of the first six natural frequencies of the frame is determined and compared with the frequency of the main excitation source of the machine to determine the rationality of the frame design. On the premise of simplifying the inter-plant obstacle avoidance mechanism into a two-dimensional model for kinematics analysis, the motion parameters of the key components of the machine were determined. At the same time, the virtual kinematics simulation single-factor test of the designed inter-plant obstacle avoidance device was carried out with the help of ADAMS 2020 software. Through the reduction in and calculation of the motion trajectory of the simulation test, it was finally determined that the forward speed of the machine, the elastic coefficient of the reset spring and the compression speed of the hydraulic cylinder were the main influencing factors of the inter-plant obstacle avoidance mower. The orthogonal test was designed and the optimal solution of the three test factors was determined. The optimal solution is taken for further field test verification. The results show that when the tractor forward speed is 1.5 km·h^{-1}, the hydraulic cylinder compression speed is 225 mm·s^{-1}, and the elastic coefficient of the reset spring is 29 N·mm^{-1}, the average leakage rate between the orchard plants is 7.64%, and the obstacle avoidance pass rate is 100%. The working stability is strong and meets the design requirements.

Keywords: obstacle avoidance between plants; lawn mower; optimal solution; trunk orchard

check for updates

Citation: Yang, Y.; He, Y.; Tang, Z.; Zhang, H. Design and Experiment of Obstacle Avoidance Mower in Orchard. *Agriculture* **2024**, *14*, 2099. https://doi.org/10.3390/agriculture14122099

Academic Editor: Maohua Xiao

Received: 14 September 2024
Revised: 18 October 2024
Accepted: 13 November 2024
Published: 21 November 2024

Copyright: © 2024 by the authors. Licensee MDPI, Basel, Switzerland. This article is an open access article distributed under the terms and conditions of the Creative Commons Attribution (CC BY) license (https://creativecommons.org/licenses/by/4.0/).

1. Introduction

With the continuous expansion of the planting scale and planting area of the forest and fruit industry in Xinjiang, by the end of 2019, the annual output of fruit in Xinjiang was 10.1 million tons, and the annual output value of the forest and fruit industry was about CNY 70 billion, accounting for more than one-quarter of the per capita net income of farmers in the whole region [1]. While increasing the economic income of the people in the whole region, it also made a significant contribution to the sustainable development of economic science in the whole region. The standardized orchard planting mode in Xinjiang

is the main trunk cultivation mode. The main characteristics of the trunk orchard are 4.0 × 2 m and 4.0 × 1.5 m row spacing. The trunk height is 60 cm, and there are 5–7 main branches on the trunk. Each main branch grows around and can fully shine on the sun. While improving the economic level of Xinjiang and the economic income of farmers, the problem of orchard grass damage is becoming more and more serious. Orchard weeds have strong vitality and wide coverage. Orchard weeds will compete with fruit trees for fertilizer, water, and interfere with the photosynthesis of fruit trees, reducing the yield of fruit trees and causing great distress to farmers in orchard management [2].

The research on the weeding technology of orchard machinery in foreign countries began in the 1950s. After long-term research and experiments, foreign weeding machinery tests has also tried out orchard special weeding machinery in addition to ordinary micro-tillers. The SILVA suspended orchard obstacle avoidance rotary cultivator produced by the Maschio company in Italy has the ideal tillage efficiency, but at the same time, its cost is high and the efficiency of inter-row operation is poor. There are many missing areas [3,4]. The 9GZ-211-type riding orchard lawn mower developed by Tsui Shui Company in Japan [5,6] has stable performance and high efficiency, but it cannot carry out inter-plant obstacle avoidance lawn mower operation. Research on obstacle avoidance mowers in China started relatively late. At present, the common weeding methods in orchards in China include chemical weeding, mechanical weeding, artificial weeding, and thermal and electrical weeding [7]. Chemical weeding is relatively clean, but it will cause damage to the ecological environment [8,9]. Artificial weeding is more thorough, but the efficiency is low and the intensity is high. With the emergence of mechanical weeding, domestic agricultural machinery production enterprises, scientific research units and agricultural colleges and universities began to carry out related research. Professor Yang's team at Northwest Agriculture and Forestry University has developed a cantilever three-disc orchard obstacle avoidance mower [10]. This mower can achieve inter-plant obstacle avoidance mowing, but the stability has been improved. The 3ZP-1600 apple intertill mower developed by the Yantai Institute of Agricultural Machinery Science [11] has the function of adjustable tillage width, but the leakage rate is high.

Affected by many factors such as climate and planting environment, China's orchard planting model is different from other countries. The overall design and operation effect of the weeding machinery designed and used abroad is not consistent with China's orchard planting model. At the same time, the design accuracy of some devices is relatively high, and it is currently used less in China. Aiming at the problems of the unreasonable design of parts, uneven force, low working efficiency, high leakage rate, poor profiling ability and unstable movement of the mower studied in China at this stage, combined with the working principle of a rotary cultivator, under the premise of adapting to the planting mode of Xinjiang trunk orchards and the operation demand of large agriculture, a trunk orchard inter-row obstacle avoidance mower is designed. This machine combines an inter-row obstacle avoidance mower with a load sensing hydraulic system with the inter-row mower and completes the work of the inter-row obstacle avoidance mower efficiently on the premise of ensuring that the skin of fruit trees is not damaged and affecting the growth and development of fruit trees. To a large extent, it solves the problem of yield reduction and labor intensity caused by the inability to remove weeds between orchards.

2. The Structure and Working Principle of Lawn Mower

2.1. Overall Structure

The main orchard obstacle avoidance mower is mainly composed of a hydraulic control system, mowing device and obstacle avoidance device. Each part is connected by the frame and connected to the tractor through a three-point suspension device. The structure diagram of the whole machine is shown in Figure 1 below. The power is transmitted from the output shaft of the tractor to the gearbox of the machine and then transferred to the side straight gearbox and the hydraulic control system after the gearbox bevel gear is converted, and then the inter-row mowing and inter-row obstacle avoidance mowing are carried out.

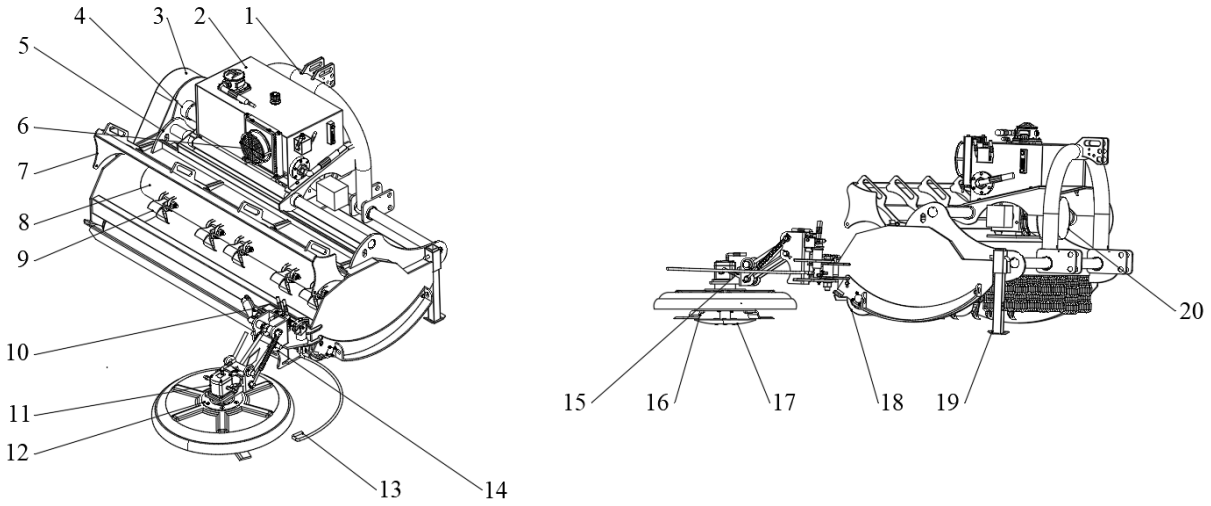

Figure 1. The overall structure diagram of the orchard inter-plant obstacle avoidance mower. 1: Suspension device; 2: hydraulic oil tank; 3: transmission belt shell; 4: belt pulley drive shaft; 5: cylindrical guide rail; 6: cooling fan; 7: frame; 8: lawn mower roller; 9: lawn mower; 10: telescopic rod; 11: hydraulic directional valve; 12: obstacle avoidance disc; 13: obstacle avoidance rod; 14: spring; 15: obstacle avoidance disc bracket; 16: inter-row mower; 17: protective disc; 18: pressing roller; 19: stent; 20: gear box.

2.2. Working Principle of Mower

Before the orchard mowing operation, the mower adopts three-point suspension to connect with the tractor. At the same time, the rear output shaft of the tractor is connected with the input shaft of the gearbox through the universal shaft, and the tractor traction mower carries out the orchard mowing operation.

After entering the orchard, the tractor's hydraulic device controls the machine to drop to the working state of the rack on the ground. During the operation, the power transmitted to the gearbox of the mower is distributed to the side drive shaft, which drives the inter-row mower device and the inter-row obstacle avoidance disc to work. The Y-type flail rotates clockwise with the knife roller at a high speed to crush the weeds. The outside of the mower is provided with a protective cover, which can effectively prevent the grass debris from splashing. The rear of the mower mechanism is provided with a pressing roller, which can effectively turn the grass and soil to play the role of green manure [12]. The inter-row obstacle avoidance device is controlled by the hydraulic system. When the obstacle avoidance rod touches the fruit tree or obstacle, the hydraulic cylinder starts to work and drives the obstacle avoidance disc to shrink for inter-row obstacle avoidance. At the same time, the mower moves horizontally along the left side perpendicular to the forward direction of the unit so as to avoid the occurrence of tree damage [13]. After the obstacle avoidance is completed, the obstacle avoidance disc returns to the extended state and continues to mow between plants. When the obstacle avoidance rod does not touch the obstacle, the obstacle avoidance system does not work, and the lawn mower normally performs inter-row mowing operations.

The power of the mowing machine is provided by the tractor to the gearbox through the universal shaft, and then the power distribution is carried out by the gearbox. One power will be transmitted to the side straight gearbox through side shaft I and then determined by the side gear transmission to meet the speed required for inter-row mowing operations and act on the cutter roller drive the cutter roller and the cutter connected to the cutter roller to carry out high-speed rotation to carry out inter-row mowing operations; at the same time, the gearbox transmits another power to the hydraulic control system of the inter-plant obstacle avoidance device through side shaft II, and the hydraulic control

system provides power to drive the hydraulic power components to complete the inter-plant obstacle avoidance mowing operation (Figure 2).

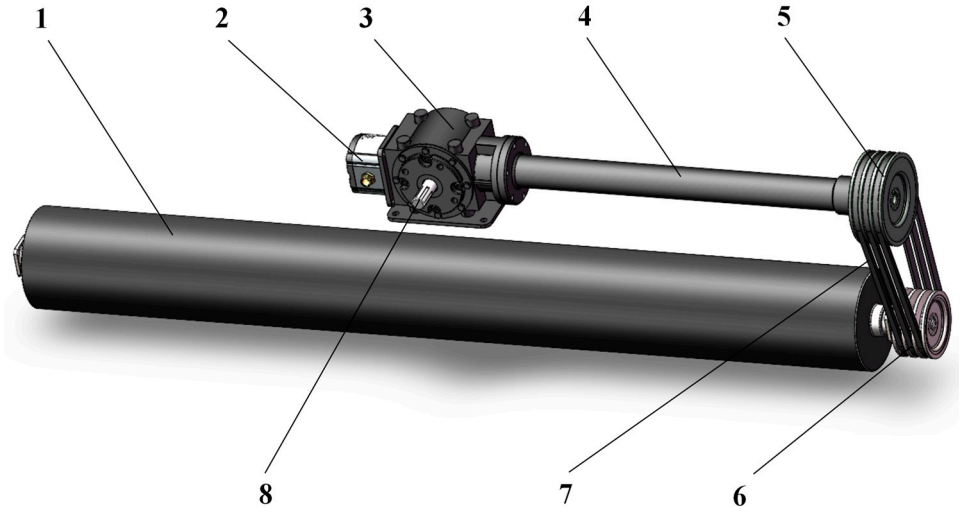

Figure 2. Transmission system diagram of mower. 1. Mowing roller. 2. Hydraulic pump. 3. Transfer box. 4. Transmission shaft. 5. Drive pulley. 6. Drive pulley. 7. Belt. 8. Input shaft.

2.3. The Main Design Parameters of Mower

The power of the main orchard inter-row obstacle avoidance mower is derived from the power output shaft of the tractor. The power required by the mower is mainly consumed in the advancement of the whole unit, the cutting tool for inter-row and inter-row stubble and the driving of the mower. Refer to the agricultural machinery design manual [14]; that is, the total power required for the mower operating unit is

$$N = N_1 + N_2 + N_3 \tag{1}$$

where the total power required by N—the operation unit, Kw; N_1—unit rolling power consumption, Kw; the power consumed by N_2—the cutter rod device, Kw; and N_3—the power consumed by transmission, Kw.

$$N = N_1 + N_2 = \frac{(F_1 + F_2)V}{1000} \tag{2}$$

In the formula, F_1—work unit rolling resistance, N; F_2—cutter stick device resistance, N; and v—operating unit working speed, $m \cdot s^{-1}$.

The rolling resistance of the working unit is calculated according to the following formula:

$$F_1 = 9.8f \cdot G \tag{3}$$

In the formula, f—the rolling friction coefficient of the working unit; and G—operating unit mass, kg.

According to the results of the machine design and analysis, analogy estimation method and agricultural machinery manual, the rolling friction coefficient is 0.3, the mass of the working unit G is 600 kg, the resistance of the cutter roller device F_2 = 5000~7000 N (analogy to the working resistance of the three disc mower), the working speed V = 2.0 $m \cdot s^{-1}$, and N_3 = 0.585 N, and the traction power Nρ of the working unit can be calculated according to Formulas (2) and (3). The range is 13.528~17.528 Kw. The total power required by the mower operation unit is calculated to be 32.59–42.24 Kw by introducing Formula (1). There are certain requirements for the tractor during orchard operation, so the tractor with a power of 44.1 Kw and above can be selected for the mowing operation.

Taking the standard trunk orchard with a row spacing of 3–5 m and plant spacing of 1.5–2.5 m as the design reference of the machine [15], the main working width of the machine is designed to be 2.1 m. The working speed of the mower is determined to be 1.5~3 km·h^{-1} according to the ground condition of the specific trunk orchard, and the working productivity, W, of the mower can be calculated, that is [16]

$$W = 0.1Bv \quad (4)$$

In the formula, W—unit theoretical productivity, hm^2·h^{-1}; B—unit structure width, m; and v—unit's theoretical speed, km·h^{-1}.

The working width of the lawn mower is B = 2.1 m. When the inter-plant obstacle avoidance lawn mower is carried out, the moving speed of the machine has a certain influence on the effect of inter-plant lawn mower. Therefore, according to the actual working environment of the orchard inter-plant obstacle avoidance lawn mower, the theoretical forward speed of the unit is determined to be 1.5 km·h^{-1} at the lowest and 3 km·h^{-1} at the highest; that is, v = 1.5~3 km·h^{-1} is taken here. Formula (4) can be used to calculate that the theoretical productivity range of the machine is 0.315~0.63 hm^2·h^{-1}. The design parameters of the main orchard obstacle avoidance mower are shown in Table 1.

Table 1. Main design technical parameters of mower.

Item	Parameter
Dimension (length × width × height)/mm	2100 × 1900 × 1000
Matching power/Kw	44.1
Structure mass/kg	600
Working width m	2.1
Operating productivity hm^2·h^{-1}	0.315~0.63
Matching tractor output shaft speed r·min^{-1}	540
Cutter roller speed r·min^{-1}	202.5
Cutter type	Y-type knife
Hang	Three-point hitch

3. Design and Simulation of Key Components of Mower

3.1. Design of Mowing Device

Because the cutting process of the weed by the mowing device is a non-fulcrum cutting, the force and material selection of the cutter become the key to ensure the efficiency of mowing. According to the shape, the cutting knife can be divided into the hammer claw type, straight-type knife, Y-type knife, L-type knife and so on. The hammer claw cutter has good crushing performance, but it requires large power and has high requirements for tractor adaptability. The structure of the straight cutter and L-cutter is simple; the power consumption is small, but the cost is high. The Y-shaped cutter has the advantages of having several cutter types at the same time, and it also has good pick-up [17]. Moreover, the symmetry of the blade increases the stability during the mowing operation. Therefore, the Y-shaped cutter is further optimized based on the selection of the Y-shaped cutter.

The thickness of the reamer is generally 6~8 mm [18]. Considering the problem of reduced work efficiency that may be caused by tool change, in order to improve the service life of the reamer, the bionic design of the reamer is carried out and the thickness of the reamer is finally determined to be 8 mm. When designing the width of the cutter, it is necessary to take into account the deformation of the force during the mowing process. In general, the width of the blade is between 30 and 100 mm [19]. Under the premise of ensuring that the deformation of the cutter is small and does not affect the quality of the work, the width of the cutter is designed to be 35 mm; referring to the conclusion that the picking effect is the best when the bending angle of the L-shaped knife is 135° determined by the comparative test of teacher Liu from Jiangsu Agriculture and Forestry Vocational and Technical College [20], the bending angle of the mower is determined to be 135°. Finally,

the total length of the Y-shaped cutter is 130 mm, the cutting width is 35 mm, the blade thickness is 8 mm, the bending radius is 45 mm, and the bending angle is 135°.

3.1.1. Cutter Arrangement Selection

The arrangement of the cutter depends on the arrangement of the pin shaft on the cutter roller. The arrangement of the pin shaft is diverse and needs to be selected according to the specific working state. The common arrangement of the pin shaft on the roller shaft [21] is shown in Figure 3 below.

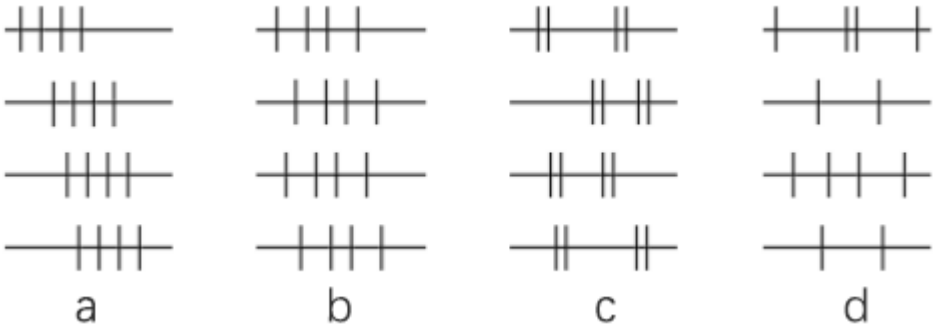

Figure 3. The arrangement of pins on the roller shaft. (**a**) Helix arrangement. (**b**) Symmetrical arrangement. (**c**) Interlaced arrangement. (**d**) Symmetrical staggered arrangement.

Spiral arrangement: The spiral arrangement has two arrangement modes: single spiral and double spiral. Figure 3a shows a single-spiral arrangement. The arrangement is simple, non-repetitive, and produces fewer leakage cuts.

Symmetrical arrangement: Figure 3b shows symmetrical arrangement. In this arrangement, the blade on the pin shaft is symmetrically installed, and the blade trajectory will be repeated, so that the blade wear is serious during the working process.

Interlaced arrangement: There are two kinds of staggered arrangement: single-chip staggered arrangement and double-chip staggered arrangement. Figure 3c shows a double-chip staggered arrangement, and it is easy to produce the card grass phenomenon during the working process.

Symmetrical staggered arrangement: Figure 3d is a symmetrical staggered arrangement. The arrangement of the blades is symmetrically arranged on the left and right sides. The trajectory is relatively uniform, and the trajectory covers a wide area, but the cost is high.

Considering that the cutter roller of the mower adopts the spiral arrangement method, the design of this method is the most simple and the leakage rate is low.

3.1.2. Cutter Statics Analysis

After the design of the whole machine of the orchard inter-plant obstacle avoidance mower, it is also necessary to design the parameters and optimize the structure of the key working parts of the mower. The blade is one of the key components of the mower. Its main function is to cut weeds and crush weeds and other debris. The strength value of the blade will become larger when it is working. If the blade breaks during the working process, the working efficiency of the machine and the quality of the broken grass will decrease. Therefore, in order to verify whether the strength of the blade selected by the mower meets the work requirements, the finite element analysis of the blade of the mower is needed [22]. Through the finite element simulation analysis, the maximum stress, strain value and the maximum deformation of the blade during the working process of the mower blade are obtained, and the simulation results are used to judge whether the design of the mower blade meets the working strength requirements.

The specific shape and size of the Y-type flail knife are established by the three-dimensional drawing software Solidworks 2018, and the format is saved as.x_t. In the

data conversion interface, the three-dimensional model is imported into the finite element simulation software ANSYS19.2 Workbench for a static simulation analysis of the blade. The material properties and parameters of the selected blade are shown in Table 2 below.

Table 2. Blade performance parameters.

Material Properties	Yield Limit/MPa	Tensile Strength/MPa	Poisson Ratio	Young's Modulus	Elastic Modulus/Mpa	Density/(kg·m^{-3})
65 Mn	430	735	0.21	198,600	1.97×10^5	7810

The Y-cutter is meshed [23], and the unit size is set to 5mm.After meshing, a total of 4033 nodes and 1988 units are generated. The meshed cutter is shown in Figure 4 below.

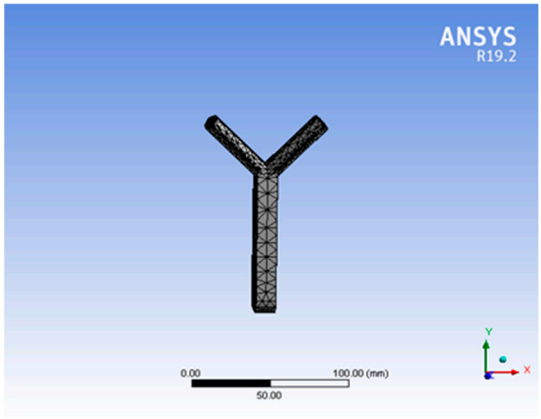

Figure 4. Cutter meshing diagram.

Through the simulation, the maximum force of the cutter during the operation is measured. When the measured weed suitability force is in the range of 6.0 to 16.8 N per millimeter, and the static analysis of the cutter is carried out after the constraint is added at the connection of the knife hole. Through the ANSYS Workbench software simulation, the equivalent elastic deformation cloud map, displacement deformation cloud map, and stress deformation cloud map of the cutter are obtained, as shown in Figure 5 below.

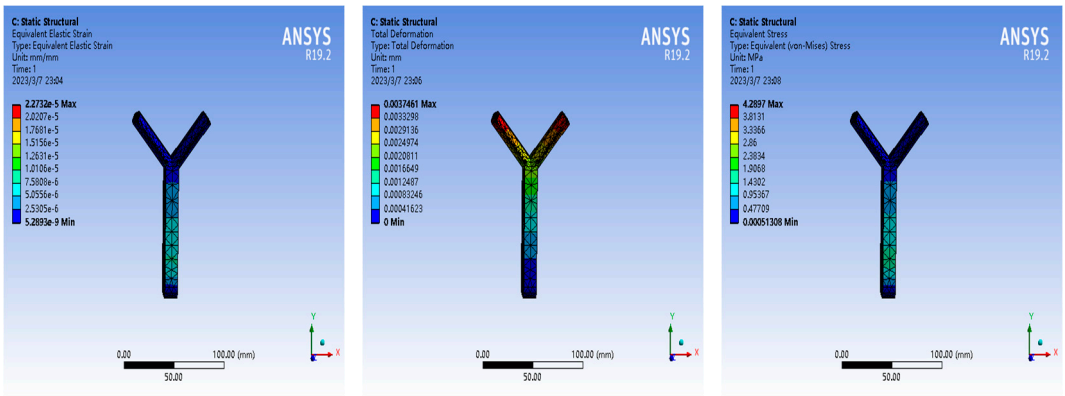

(**a**) (**b**) (**c**)

Figure 5. Cutter statics simulation results. (**a**) Equivalent elastic deformation cloud diagram of cutter. (**b**) Cutter displacement deformation cloud map. (**c**) Cutter stress deformation cloud diagram.

From the equivalent elastic deformation cloud diagram of the cutter in Figure 5a, it can be concluded that the maximum equivalent elastic deformation value of the cutter is 2.273×10^{-5} mm, and the equivalent elastic deformation range of the cutter is

5.289×10^{-8}~2.273×10^{-5} mm. It can be concluded from the displacement deformation cloud diagram of the cutter in Figure 5b that the maximum displacement deformation of the cutter is 3.74×10^{-3} mm, and the maximum displacement deformation occurs in the blade part. This is because the blade is the main working part of the cutter, and it is relatively large in the process of mowing. In the actual work, the displacement deformation is small, which will not affect the normal operation of the cutter. From the stress deformation cloud diagram of the cutter in Figure 5c, it can be concluded that the maximum stress of the cutter is 4.289 MPa, which is far less than the allowable stress value (430 MPa) of the selected material, so the strength design of the cutter meets the operation requirements.

3.1.3. Kinematics Analysis of Cutter

The motion trajectory of the cutter is a combination of circular motion and linear motion when mowing; that is, the motion trajectory of any point on the cutter is a regular cycloid [24,25]. The center of the cutter roll rotation is taken as the origin of the coordinate. The forward direction of the mower is the *x*-axis, and the vertical plane of the *x*-axis is the *y*-axis. The motion trajectory of the cutter is simulated. In the figure, R is the rotation radius of the cutter, ω is the angular velocity of the cutter roll, and Vm is the forward speed of the machine. The motion trajectory of the cutter is shown in Figure 6 below.

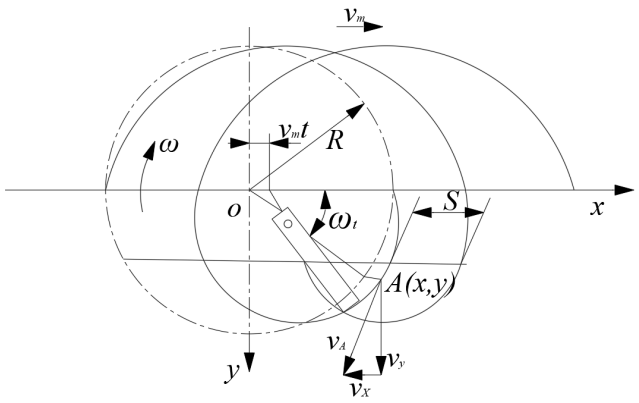

Figure 6. Cutter trajectory diagram.

From the trajectory diagram of the upper cutter, it can be seen that when the Y-cutter begins to move, it coincides with the *X*-axis of the trajectory. When the movement time is t, the coordinate equation of the position of the endpoint of the cutter can be expressed as follows:

$$x = R \cdot \cos \omega t + v_m t \tag{5}$$

$$y = R \cdot \sin \omega t \tag{6}$$

In the formula, R—Y cutter rotation radius, mm;
ω—cutter angular velocity, $r \cdot min^{-1}$;
v_m—machine forward speed, $m \cdot s^{-1}$.
The velocity of the cutter endpoint in the *x*-axis and *y*-axis is

$$v_x = d_x/d_t = v_m - R\omega sin\omega t \tag{7}$$

$$v_y = d_y/d_t = R\omega cos\omega t \tag{8}$$

The absolute motion speed of the cutter is

$$v_A = \sqrt{v_X^2 + v_y^2} = \sqrt{v_m^2 + R^2\omega^2 - 2v_m R\omega sin\omega t} \tag{9}$$

According to the relevant literature, the minimum limit speed of the blade of the mower is 30 $m \cdot s^{-1}$ when the mower is in the unsupported high-speed rotary mower

operation. In order to ensure the normal mower operation, the cutting speed of the mower device needs to be greater than the minimum limit speed [26], so the speed of the cutter shaft is

$$n = \frac{30(v_A + v_m)}{\pi r} \tag{10}$$

Quorum: $r = \frac{D}{2-h}$, $h = \frac{\pi D v_m}{m v_A}$.

In this type, D—the cutter roller diameter, mm; h—the cutter blade length, mm; and m—the number of cutters, put.

Furthermore, it can be calculated that the conditions for the mower to not miss cutting are

$$\frac{v_A}{v_m} \geq \frac{2\pi r}{mh} \tag{11}$$

3.2. Modal Analysis of Mower Frame

The frame of orchard obstacle avoidance mower is the key component of bearing and supporting the mower device, hydraulic cylinder, inter-row obstacle avoidance device and soil-covering roller. When the external excitation frequency is close to the inherent excitation frequency of the frame, the resonance of the frame will be caused. If the key components of the mower are seriously damaged under the strong vibration, the working performance of the machine will be affected. Through the finite element modal analysis of the frame, the rationality of the frame design is verified.

The three-dimensional model of the frame is shown in Figure 7, which is composed of a front beam, a middle beam, a rear beam and two side plates.

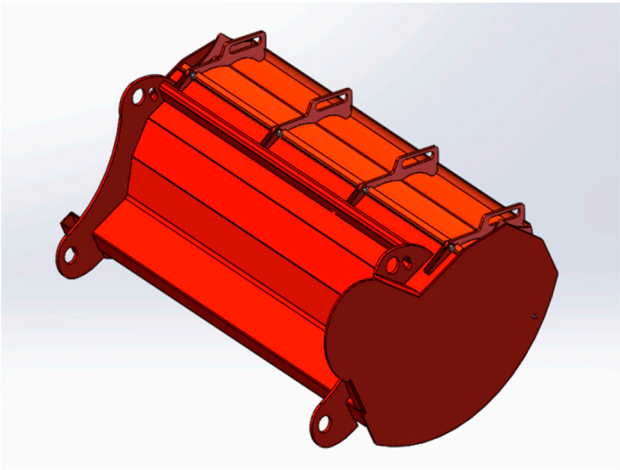

Figure 7. Three-dimensional model of frame.

3.2.1. Frame Model Parameters

The simplified frame is a rigid connection model, which is saved as.x_t format and imported into ANSYS Workbench. In this frame, Q235 structural steel with good plasticity, good strength and a relatively cheap price is selected. The frame model parameters are shown in Table 3.

Table 3. Rack model parameters.

Frame Size/mm	Material Properties	Tensile Strength/MPa	Poisson Ratio	Yield Limit/ MPa	Density/ (kg·m^{-3})	Elastic Modulus/ MPa
1600 × 820 × 600	Q235	450	0.3	235	7850	2.10 × 10^5

3.2.2. Meshing

Before the modal analysis of the frame, the frame needs to be meshed to ensure the reliability of the simulation results. When meshing, the unit size is set to 10 mm. After meshing, a total of 150,597 nodes are generated, and the number of units is 74,241. The rack meshing model is shown in Figure 8 below.

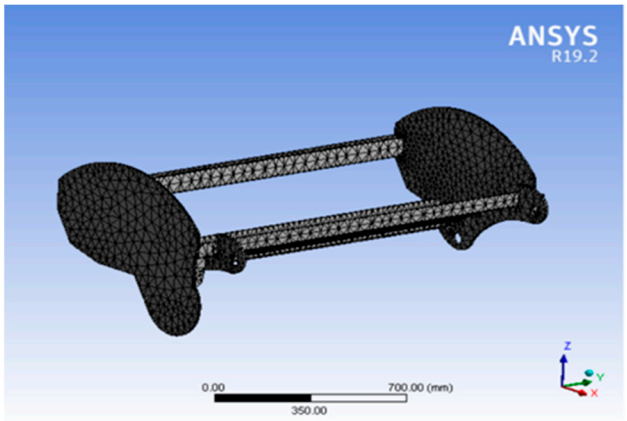

Figure 8. Frame finite element model.

3.2.3. Rack Simulation Result Analysis

The stability of the general machine during the mowing operation mainly depends on the low-order modal characteristics [27,28]. Therefore, only the first six-order modal frequency and vibration mode analyses are carried out here. The first six-order modal vibration modes are shown in Figure 9a–f, and the natural frequency and vibration mode changes are shown in Table 4.

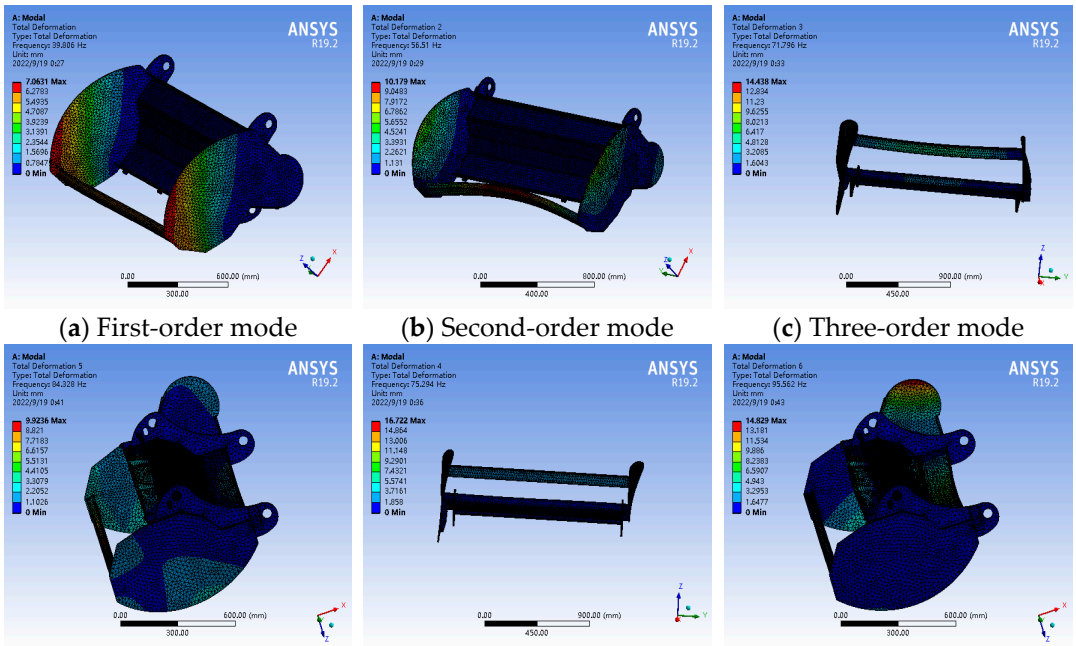

(**a**) First-order mode (**b**) Second-order mode (**c**) Three-order mode

(**d**) Fourth-order mode (**e**) Fifth-order mode (**f**) Sixth-order mode

Figure 9. Frame of the first six-order modal analysis diagram.

According to the analysis of the first six-order vibration mode cloud diagram of the frame, the main deformation parts of the frame are the rear beam and the two side plates. The main reason is that there are many support points of the front beam and the middle

beam, which makes the overall stiffness of the front end of the frame larger, and the support points of the rear beam are fewer, and the span is large, so the stiffness is small and easy to deform. The two sides of the plate extend forward and back ward for a long time, resulting in too large deflection and easy deformation. A longitudinal beam can be added between the two beams to further improve the rigidity of the mower frame.

Table 4. Results of the first six-order modal analysis of the frame.

Order	Natural Frequency/Hz	Vibration Mode Description	Maximum Deflection/mm
1	39.806	The two sides of the plate are twisted left and right	7.0613
2	56.51	Rear crossbeam sunken, side plate twisted	10.179
3	71.796	The rear crossbeam bends outwards	14.458
4	75.294	The two sides of the plate are bent inward	16.722
5	84.328	The middle beam is raised upwards	9.9236
6	95.562	The front beam bends inward, and the upper beam bulges upward.	14.829

From Table 4, it can be concluded that the natural frequency range of the frame is 39.806~95.562 Hz. The working frequency of the obstacle avoidance mower in the trunk orchard can be determined by the actual working speed of the mower [29]:

$$f = \frac{\omega}{2\pi} = \frac{n}{60} \tag{12}$$

where in f—the operating frequency of the excitation source, Hz; and n—the actual working speed of the excitation source, r·min^{-1}.

Regarding the obstacle avoidance mower in the orchard used to avoid obstacles in the process of mowing operations, the main external excitation sources are as follows: the unevenness of the orchard, mowing shaft, obstacle avoidance device, transmission system and tractor output shaft generated by the vibration. The obstacle avoidance device is an independent part. When the mowing operation is stable, the excitation force is small, and the flatness of the trunk orchard in Xinjiang is relatively high. Therefore, the excitation caused by the obstacle avoidance device and the unevenness of the orchard can be ignored.

Taking the rotation speed of the cutter roller as 202.5 r·min^{-1}, the maximum excitation frequency of the cutter roller can be calculated to be 3.38 Hz by taking the above formula. The rotation speed of the power output shaft of the tractor is 540 r·min^{-1}, and the maximum excitation frequency is 8.6 Hz. It can be concluded that the main excitation source of the frame is the vibration of the output shaft of the tractor, and the excitation frequency value is not within the inherent frequency range of the frame of 39.806~95.562 Hz [30], so it will not resonate with the frame during operation. The frame works stably and reliably, and the lawn mower can carry out normal inter-plant obstacle avoidance mowing operations.

4. Design and Simulation of Automatic Obstacle Avoidance Device Among Three Plants

4.1. The Structure Design of Automatic Obstacle Avoidance Device Between Plants

In order to solve the problem of high labor intensity and high cost caused by the difficulty of inter-plant mowing in the main orchard, an automatic obstacle avoidance mowing device was designed. The device can realize inter-plant mowing without damaging the tree. The device is mainly composed of a cutter head, hydraulic motor, hydraulic cylinder, obstacle avoidance rod, fixed plate and so on. The automatic obstacle avoidance device between plants is shown in Figure 10 below.

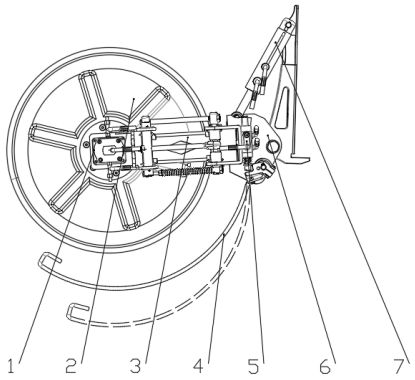

Figure 10. Automatic obstacle avoidance device between plants. 1. Hydraulic motor. 2. Cutterhead. 3. Connecting shaft. 4. Breakthrough rod. 5. Control valve. 6. Connecting plate. 7. Cylinder.

The obstacle avoidance device between the plants is supported by the connecting plate, and the pin is connected to the side of the mower frame. The obstacle avoidance plate between the plants is controlled by the hydraulic system to work. When the orchard mowing operation is carried out, under the action of the hydraulic cylinder, the mowing cutter head is extended into the plants to carry out the inter-plant mowing operation. When the obstacle avoidance rod touches the fruit tree, the pressure control valve drives the hydraulic control system to work, the hydraulic cylinder shrinks and then drives the mowing cutter head to shrink medially to complete an inter-plant obstacle avoidance mowing operation. In the process of a mowing operation, the obstacle avoidance plate and the fruit tree are in relative motion. When the motion speed does not reach a stable state, it is easy to cause tree damage and low work efficiency. In order to avoid this situation, after reading the relevant literature and theoretical analysis, it is proposed to design the obstacle avoidance rod as an arc. Under this design, the obstacle avoidance rod can normally perform inter-row obstacle avoidance mowing under multi-party pressure. In order to determine the specific motion parameters of the obstacle avoidance disc, it is necessary to simplify the inter-plant obstacle avoidance mechanism into a two-dimensional model for kinematic analysis. The motion diagram of the inter-plant automatic obstacle avoidance device is shown in Figure 11 below:

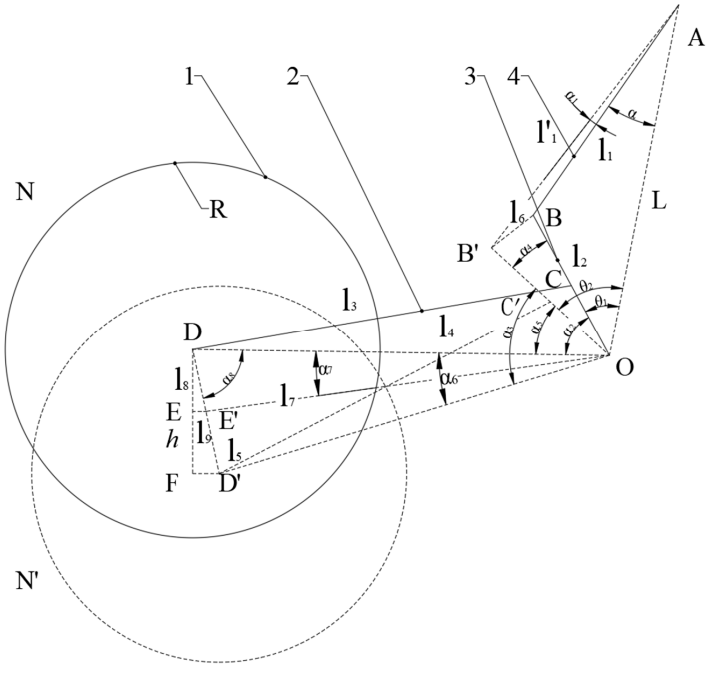

Figure 11. Motion diagram of automatic obstacle avoidance device between plants. 1. Cutterhead. 2. Cutterhead connecting plate. 3. Connecting plate. 4. Hydraulic cylinder. Note: N is the position of

the cutter head under the compression state of the hydraulic cylinder; n′ is the position of the cutter head in the elongation state of the hydraulic cylinder; R is the radius of the cutter head and the length of the hydraulic cylinder in the compressed state; l_1 is the length of the hydraulic cylinder in compression state. l_1 the length of the hydraulic cylinder in the telescopic state; L is the distance between the position of the hydraulic cylinder and the connecting plate; l_3 is the position of both ends of the connecting plate; l_4 is the distance between the midpoint of the cutter connection plate of the cutter head; l_5 is the distance between the center of the cutter head in the two middle states; l_6 is the distance between the two connection points in two states; l_7 is the distance between point O and E′; l_8 is the distance between two points of DE; l_9 is the distance between EE′; α is the angle between OA and AB; α_1 is the angle between BA and B′A; θ_1 is the angle between OA and OB. θ_2 is the angle between OA and OB′; α_2 is the angle between OD and OB; α_3 is the angle between OD′ and OB′; α_4 is the angle between OB and OB′; α_5 is the angle between OD and OB′; α_6 is the angle between OD and OD′; α_7 is the angle between OE and OD; α_8 is the angle between D′ D and OD; and h is the vertical distance between the center of the cutter head in the two states.

After analyzing the motion diagram, it can be seen that in order to ensure the normal obstacle avoidance and mowing operation of the obstacle avoidance disc, it is necessary to determine the farthest moving distance of the cutterhead. Because the movement of the cutterhead is controlled by the hydraulic cylinder, it is necessary to determine the proportional relationship between the expansion of the hydraulic cylinder and the moving distance of the cutterhead. Through the analysis of the motion process of the lawn mower, it can be seen that AB and DC are fixed parts, so the length and some related angle values formed during the motion process are unchanged. After analyzing the motion diagram, the geometric relationship is as follows:

$$l_1' = l_1 + d \tag{13}$$

$$OB = OB' = l_2 \tag{14}$$

$$OD = OD' = l_4 \tag{15}$$

$$\alpha_6 = 2\alpha_7 \tag{16}$$

$$DE' = D'E' = \frac{1}{2}OE' \tag{17}$$

$$\alpha_4 + \alpha_5 = \alpha_2 = \alpha_3 = \alpha_5 + \alpha_6 \tag{18}$$

$$\Delta DEE' \sim \Delta DFD' \tag{19}$$

It can be deduced from the sine theorem that

$$\frac{E\prime O}{sin\alpha_8} = \frac{E\prime D}{sin\alpha_7} \tag{20}$$

In ΔOBA, $\Delta ABB'$, $\Delta OAB'$, $\Delta ODD'$, $\Delta BOB'$, $\Delta DEO'$, it can be deduced from the cosine theorem that

$$l_2^2 = {l_1'}^2 + L^2 - 2{l_1'}^2 Lcos(\alpha + \alpha_1) \tag{21}$$

$$l_6^2 = 2l_2^2 - 2l_2 l_2 cos\alpha_4 \tag{22}$$

$$l_6^2 = {l_1'}^2 + l_1^2 - 2{l_1'}^2 l_1 cos\alpha_1 \tag{23}$$

$$l_4^2 = l_5^2 + l_4^2 - 2l_4 l_5 cos\alpha_8 \tag{24}$$

$$l_5^2 = l_4^2 + l_4^2 - 2l_4 l_4 cos\alpha_6 \tag{25}$$

$$l_8^2 = l_4^2 + (l_7 + l_9)^2 - 2l_4(l_7 + l_9)^2 cos\alpha_7 \tag{26}$$

In ΔDEE′, the following can be calculated by the Pythagorean theorem:

$$\left(\frac{1}{2}l_5\right)^2 + l_9^2 = l_8^2 \tag{27}$$

By ΔDEE′~ΔDFD′, the following can be launched:

$$\frac{DE}{DD'} = \frac{DE'}{FD'} \Rightarrow h = \frac{l_5^2}{2l_8^2} \tag{28}$$

In order to ensure the normal operation of the obstacle avoidance device between the plants of the lawn mower, when the hydraulic cylinder is elongated, the center of the cutting disc should be located on the center line of the fruit tree. After contraction, the vertical distance between the horizontal tangent of the cutting disc and the center line of the fruit tree is greater than the radius of the fruit tree. The design size of the lawn mower is known, which is 250 mm, 700 mm, and 60°. When the hydraulic cylinder is in a contraction state, it is determined as the initial state, which is 30°. When the hydraulic cylinder reaches the maximum position, it is 15°. The calculated elongation is 72 mm, h is 420 mm, and the measured orchard radius d is 150 mm. The change in h is more than 2 times that of the radius of the fruit tree, so it can be concluded that the mechanism can effectively reduce the damage to the fruit tree and complete the obstacle avoidance mowing operation between the plants with high efficiency.

4.2. Kinematics Simulation and Experiment of Automatic Obstacle Avoidance Device Between Plants

Through the analysis of the movement process of the inter-row obstacle avoidance mower and a review of the relevant literature, it is concluded that the size of the coverage area of the inter-row obstacle avoidance disc has a great influence on the weeding effect during the mowing operation. The main factors affecting the size of the coverage area of the inter-row obstacle avoidance disc are as follows: the forward fragmentation of the machine, the compression speed of the hydraulic cylinder, the reset spring coefficient and the diameter of the cutter. In order to determine the influence degree of each influencing factor on the designed inter-plant obstacle avoidance mowing device, the virtual kinematics simulation single-factor test of the designed inter-plant obstacle avoidance device was carried out by ADAMS [31], and the area covered by the inter-plant mowing operation of the weeding cutter head (leakage rate) was used as the single-factor test index. The simulation results provide a theoretical basis for the subsequent determination of the final test factors.

4.2.1. Establishment of Simulation Model of Automatic Obstacle Avoidance Device Between Plants

Before importing the geometric model, it is necessary to set the working environment of ADAMS [32]. First, we select the Working Grid under Settings to set the size, spacing, and direction of the grid; then, we need to set the unit. In order to simulate the trajectory of the obstacle avoidance device between plants, a simplified device model was established in SolidWorks software. Including the casing, the ground, the obstacle avoidance device and the pear tree, using the casing instead of the simplified machine model, the following applied: the width was set to 4000 mm, representing the row spacing of the orchard; the cylinder with a diameter of 40 mm and a height of 3500 mm represents the pear tree; and the distance between the two cylinders on the same side is 1500 mm, which represents the plant spacing of the pear tree. The simulation model is shown in Figure 12.

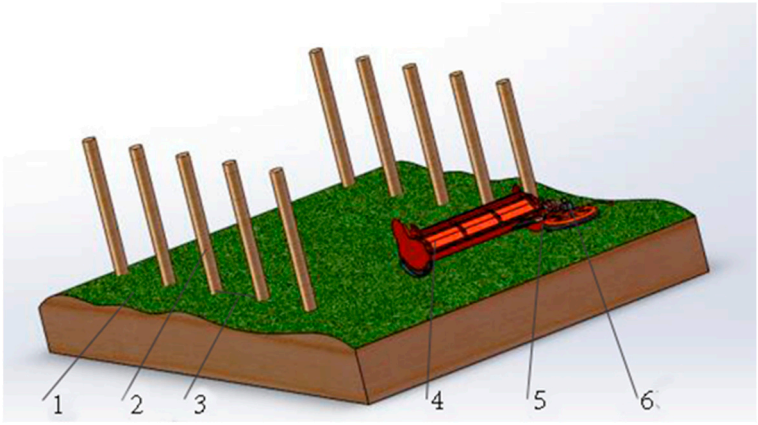

Figure 12. Simulation model of obstacle avoidance mowing device between plants. 1. Grassland 2. Pear tree. 3. Pear tree spacing. 4. Rack. 5. Barrier plate. 6. Barrier rod.

4.2.2. Kinematics Simulation of Automatic Obstacle Avoidance Device Between Plants

After each component is created by SolidWorks software, it is imported into ADAMS, and a rotating pair and a constraint pair are added between the obstacle avoidance disc and the rotating shaft [33]. The constraint relationship of the mower is shown in Figure 13.

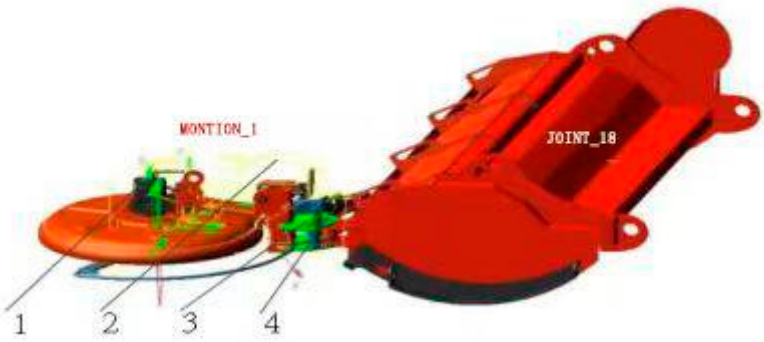

Figure 13. Constraint relationship diagram of obstacle avoidance mower between orchard plants. 1. Obstacle avoidance disc drive. 2. Fixed pair. 3. Rotating pair. 4. Axis rotation drive.

In order to verify the correctness of the model, the Model Verify module under Tools verifies the degree of freedom and constraints of the model. The model verification information is shown in Figure 14.

It can be concluded from Figure 14 that the model of obstacle avoidance and mowing device between plants is established correctly. The constraint type and number of the model are shown in Table 5.

Table 5. Constraint type and number of obstacle avoidance mower in trunk orchard.

Constraint Type	Number
Fixed pair	2
Revolute pair	5
Drive	5
Degree of freedom	9

Before the ADAMS virtual kinematics simulation single-factor test of the inter-plant obstacle avoidance mower, it is necessary to determine and set the parameters of the relevant influencing factors of the simulation model. The simulation test is mainly based

on the forward speed of the machine, the diameter of the cutter head, the compression speed of the hydraulic cylinder of the obstacle avoidance device and the elastic coefficient of the reset spring of the obstacle avoidance device. Considering the different working environment of the mower, the forward speed of the machine should be appropriate; at the same time, in order to ensure the normal inter-plant obstacle avoidance mowing operation of the obstacle avoidance disc, the sensitivity of the hydraulic system should be taken into account; the size of the cutterhead should also be moderate to ensure the removal effect of weeds between plants. On this basis, according to the characteristics of the row spacing of the trunk orchard and the field investigation, the numerical range of the influencing factors was preliminarily determined: the forward fragmentation of the machine was 1.5~2.5 km·h^{-1}, the elastic coefficient of the reset spring was 20~40, the compression speed of the hydraulic cylinder was 120~140 mm·s^{-1}, and the diameter of the cutter head was 400~440 mm.

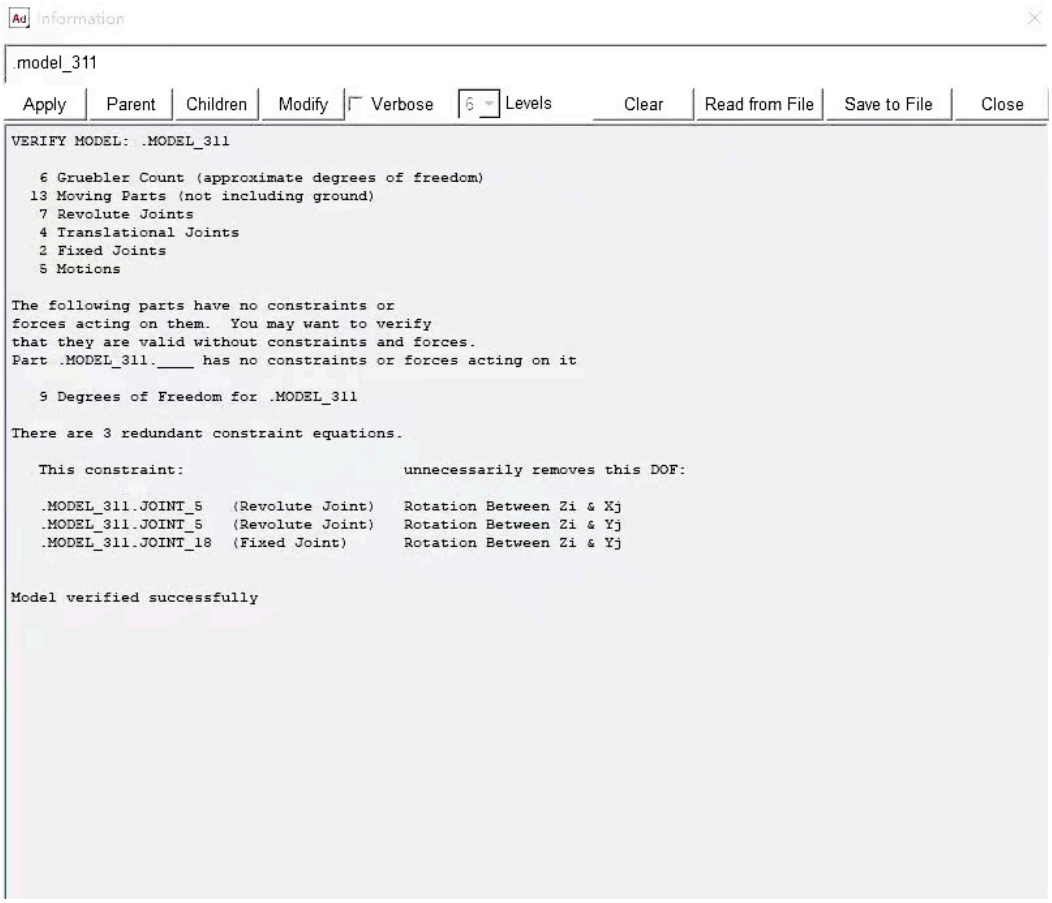

Figure 14. Model validation information.

4.2.3. Simulation Results and Experimental Analysis

After determining the scope of each influencing factor, the ADAMS software is imported to set the parameters of each influencing factor, and the mowing operation process of the inter-plant obstacle avoidance mower is drawn after post-processing. The whole process can be divided into four stages (inter-plant mowing operation, obstacle avoidance rod touching tree, inter-plant obstacle avoidance, obstacle avoidance end). The simulation process is shown in Figure 15a–d.

In order to determine the influence of each influencing factor on the efficiency of inter-plant mowing of inter-plant obstacle avoidance mower, it is proposed to take 5 values for each influencing factor, and take the leakage rate as the test index. The control variable

method is used to carry out single-factor test on each influencing factor, and the simulation results of 4 influencing factors are obtained by this method.

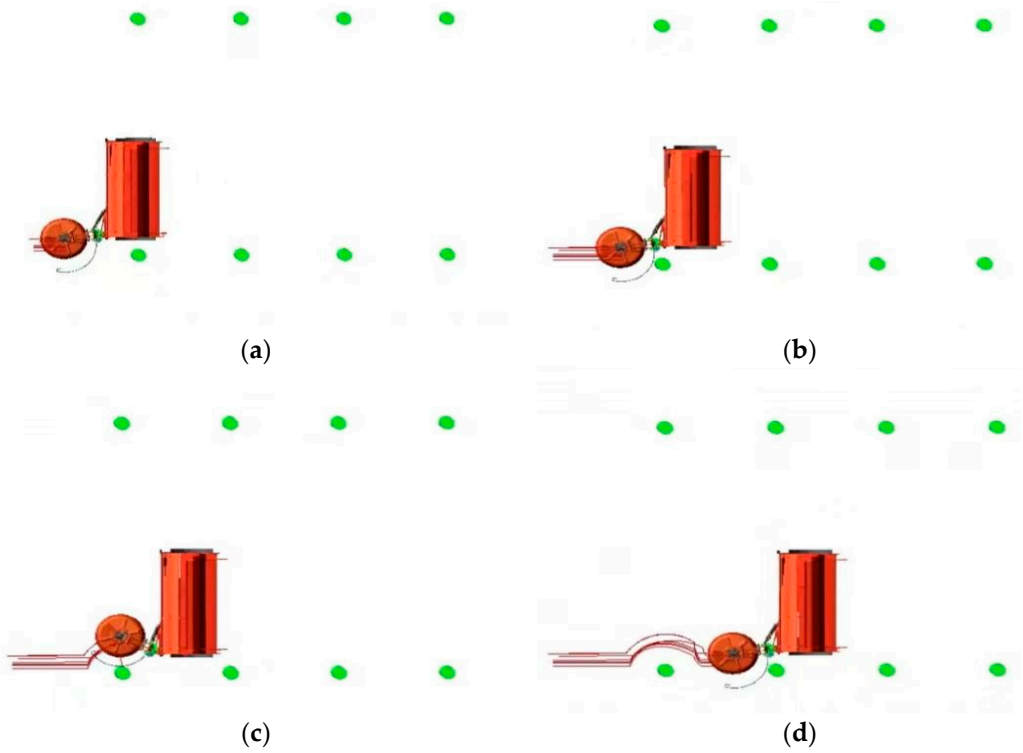

Figure 15. Simulation operation process of obstacle avoidance lawn mower in orchard. Note: (**a**): inter-row mowing operation stage; (**b**): obstacle avoidance rod touch tree stage; (**c**): inter-row obstacle avoidance stage; (**d**): obstacle avoidance end stage.

Taking the missed cutting rate as the test index, the specific representation method is as follows: a cutting area with a length of 1.5 m and a width of Lp is set, and its area becomes the total cutting area. Under the premise of the control variable method, different values are input respectively, so that the mower can pass through the cutting area, and the trace function in ADAMS Review is used to track the motion trajectory of the mower cutter, and then the trajectory is imported into Auto CAD for recovery processing [34]. The boundary of the cutting area of the cutter is extracted as shown in Figure 16. According to the area of the uncut area of the cutting area and the area of the rectangular area, the leakage rate is calculated, and then the influence size is determined according to the swing amplitude of the leakage rate, and finally the main influencing factors are determined for the test.

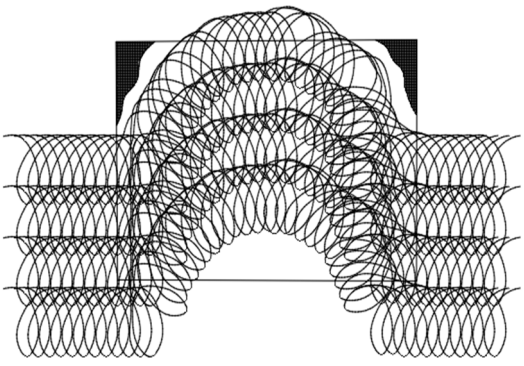

Figure 16. Area of cutter cutting area.

Under the premise of using the control variable method and using the area of the cutter cutting area to represent the test index, the influence curve of each factor on the working efficiency of the inter-row obstacle avoidance mower is shown in Figure 17a–d.

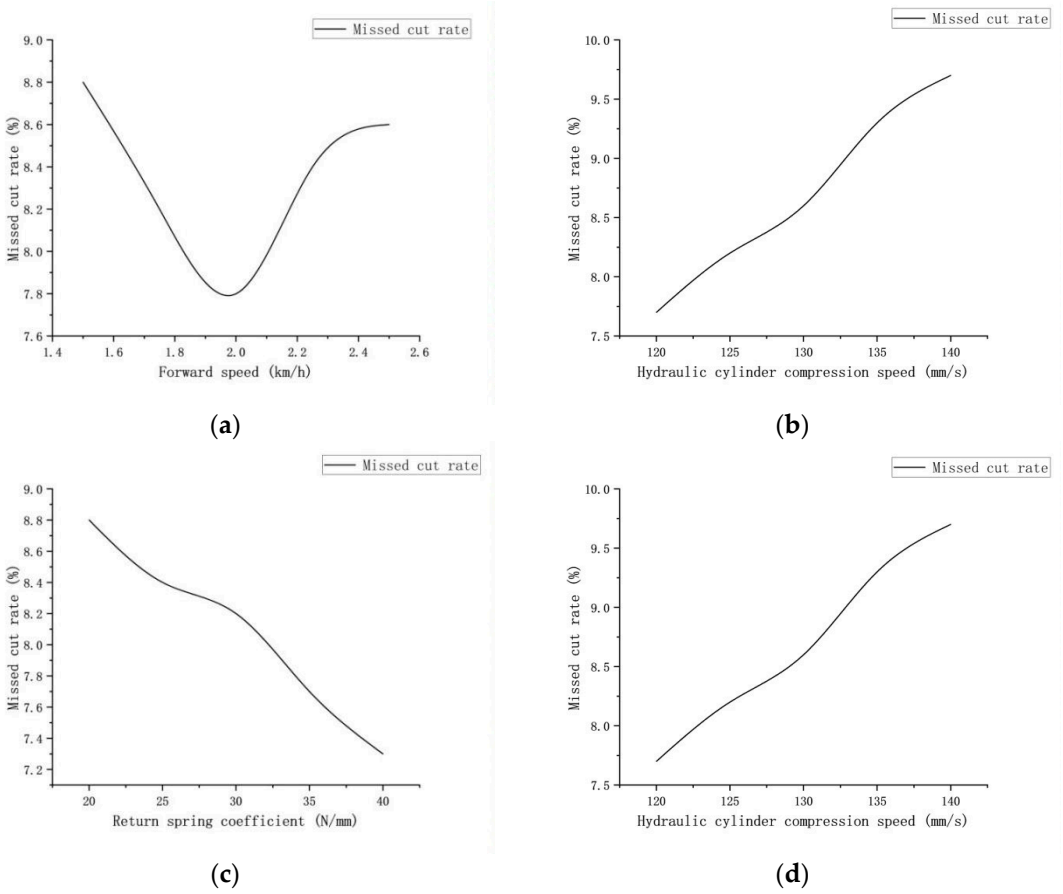

Figure 17. The influence curve of various factors on the working efficiency of the inter-plant obstacle avoidance mower. (**a**) The relationship between the forward speed of the machine and the leakage cutting rate. (**b**) The relationship between the compression speed of hydraulic cylinder and the leakage cutting rate. (**c**) Relationship between elastic coefficient of reset spring and leakage cutting rate. (**d**) The relationship between cutter diameter and leakage cutting rate.

From the analysis of the above figures, it can be seen that, within the range of the selected factors, the leakage rate decreases with the increase in the forward speed of the machine; with the increase in the compression speed of the hydraulic cylinder, the leakage rate increases. With the increase in the elastic coefficient of the reset spring, the leakage rate decreases first and then gradually stabilizes. With the increase in the diameter of the weeding cutter, the leakage rate remains almost unchanged. Therefore, compared with the other three influencing factors, it has less influence on the working efficiency of the machine. In summary, the forward speed of the machine, the elastic coefficient of the reset spring and the compression speed of the hydraulic cylinder are the main influencing factors of the inter-plant obstacle avoidance mower.

4.3. Test and Analysis of Automatic Obstacle Avoidance Device Between Plants

4.3.1. Test Factors and Indicators

The Box–Behnken experimental design is mainly used to verify the nonlinear correlation between the influencing factors and the experimental indicators. In this experiment, the three factors determined by the single-factor simulation experiment above are selected as the influencing factors, the forward speed A of the machine, the compression speed

B of the hydraulic cylinder and the elastic coefficient C of the reset spring. At the same time, each factor is set at three levels, and the factor level coding table [35,36] is determined according to Design Expert 11, as shown in Table 6 below.

Table 6. Factor level coding table.

Coded Value	Experimental Factors		
	Advancing Velocity (km·h^{-1})	Elasticity Coefficient of Reset Spring (N·mm^{-1})	Compression Speed of Hydraulic Cylinder (mm·s^{-1})
Upper level −1	1.4	25	200
Zero level 0	1.5	35	230
Lower level +1	1.6	45	260

4.3.2. Test Results

The forward speed of the machine affects the working efficiency of the mower. If the forward speed is too fast, the tree will be damaged and the rate of missed cutting will also increase. Therefore, the forward speed of the machine is set to 1.4 km·h^{-1}, 1.5 km·h^{-1} and 1.6 km·h^{-1}, respectively. The compression speed of the hydraulic cylinder also has a certain influence on the working efficiency of the inter-row obstacle avoidance device. If the compression speed is too slow, it will accelerate the wear degree of the tool while damaging the tree. If the compression speed is too fast, it will also cause the inter-row leakage rate to increase. Therefore, through the kinematics simulation test of the inter-row obstacle avoidance device, the compression speed of the hydraulic cylinder is determined to be 200 mm·s^{-1}, 230 mm·s^{-1}, and 260 mm·s^{-1}, respectively. At the same time, the size of the elastic coefficient of the reset spring also has a certain impact on the working efficiency of the inter-plant obstacle avoidance device. If the elastic coefficient of the reset spring is too large, it will lead to the phenomenon of the cutter chuck. If the elastic coefficient of the reset spring is small, the ability to resist external forces is weak, which will increase the leakage rate. Therefore, the value of the elastic coefficient of the reset spring is set to 25, 35 and 45.

The leakage rate between plants is used as the test index to verify the operation performance of the obstacle avoidance mower in the trunk orchard. The calculation formula is as follows:

$$\eta = \frac{A_1}{A_0} \times 100\% \tag{29}$$

$$A_1 = A_2 - A_3 \tag{30}$$

In the formula, η—the inter-plant leakage rate, %; A_0—the total area of test area, hm^2; A_1—the actual leakage area, hm^2; A_2—the uncut area, hm^2; and A_3—the uncultivated area, hm^2.

According to the Box–Behnken test principle, under the premise of ensuring that the machine is not damaged, the three-factor three-level central combination test principle is selected, and a total of 17 sets of tests are performed. The test plan and response values are shown in Table 7.

Table 7. Test scheme and response value.

Test	Advancing Velocity A (km·h^{-1})	Compression Speed of Hydraulic Cylinder B (mm·s^{-1})	Elasticity Coefficient of Reset Spring C (N·mm^{-1})	Targets of Test
				Leakage Rate (%) G_1
1	−1	−1	0	8.75
2	1	−1	0	6.87
3	−1	1	0	8.26
4	1	1	0	7.84
5	−1	0	−1	8.42

Table 7. *Cont.*

Test	Advancing Velocity A ($km \cdot h^{-1}$)	Compression Speed of Hydraulic Cylinder B ($mm \cdot s^{-1}$)	Elasticity Coefficient of Reset Spring C ($N \cdot mm^{-1}$)	Targets of Test
				Leakage Rate (%) G_1
6	1	0	−1	6.96
7	−1	0	1	7.95
8	1	0	1	7.02
9	0	−1	−1	6.75
10	0	1	−1	8.26
11	0	−1	1	7.55
12	0	1	1	7.62
13	0	0	0	7.87
14	0	0	0	8.18
15	0	0	0	7.84
16	0	0	0	7.75
17	0	0	0	7.73

Design Expert 11 is used to fit and analyze the experimental data in Table 7 [37], and the significance test results of the regression model of the missing rate between plants are obtained, as shown in Table 8.

Table 8. The significance test results of regression model.

Source of Variance	Quadratic Sum	Degree of Freedom	Mean Square	Ratio	Significance Level
Model	4.89	9	0.54	11.74	0.0019
A	2.75	1	2.75	59.44	0.0001
B	0.53	1	0.53	11.47	0.0117
C	7.813×10^{-3}	1	7.813×10^{-3}	0.17	0.0343
AB	0.53	1	0.53	11.52	0.0115
AC	0.070	1	0.070	1.52	0.0257
BC	0.52	1	0.52	11.21	0.0123
A^2	0.010	1	0.010	0.22	0.6527
B^2	1.918×10^{-4}	1	1.918×10^{-4}	4.147×10^{-3}	0.9505
C^2	0.47	1	0.47	10.26	0.0150
Residual error	0.32	7	0.046		
Lack of fit	0.19	3	0.064	1.96	0.2614
Error	0.13	4	0.033		
Summation	5.21	16			

Note: $p < 0.05$ indicates significant, $p < 0.01$ indicates extremely significant.

According to the significance test results of the regression model, the design model F = 11.74, and the coefficients of A, B, C, AB, AC, BC and C^2 reached a significant level. P = 0.2614 ($p > 0.01$), indicating that the regression model has a good fitting effect and the experimental design is reliable. The regression equation of the inter-row building rate of the obstacle avoidance mower in the trunk orchard is

$$Y = 61.44 - 53.26A - 0.13B + 0.31C + 0.12AB + 0.13AC - 1.2 \times 10^{-3}BC + 4.92A^2 + 7.5 \times 10^{-6}B^2 - 3.35 \times 10^{-3}C^2 \quad (31)$$

In the formula, Y—the inter-plant leakage rate, %; A—the machine forward speed, ($km \cdot h^{-1}$); B—the obstacle avoidance hydraulic cylinder compression speed, $mm \cdot s^{-1}$; and C—the reset spring elastic coefficient, $N \cdot mm^{-1}$.

4.3.3. Response Surface Results

The response surface method was used to analyze the influence of each influencing factor on the inter-plant leakage rate. The forward speed of the tractor, the elastic coefficient of the reset spring and the telescopic speed of the hydraulic cylinder were fixed at the zero level, and the interaction of the other two factors on the inter-plant leakage rate G1 was investigated. From Figure 18a, it can be analyzed that when the compression speed of the hydraulic cylinder is the intermediate horizontal value of 230 mm·s^{-1}, and the forward speed of the machine is a fixed horizontal value, the inter-plant leakage rate increases first and then decreases with the increase in the elastic coefficient of the reset spring. The main reason for this situation is that when the forward speed of the machine is relatively fast and the elastic coefficient of the reset spring is low, the automatic obstacle avoidance system is relatively sensitive, the inter-plant mowing operation time is relatively short, and the leakage rate is large. The reset spring coefficient gradually increases, and the ability to resist external forces while matching the operating speed of the machine is also enhanced. The time of mowing between plants increases and the missed cutting rate decreases. From the point of view of the degree of increase and decrease in the whole surface, in the interaction between the forward speed of the machine and the elastic coefficient of the reset spring on the inter-plant leakage rate, the elastic coefficient of the reset spring has a significant effect on the inter-plant leakage rate. It can be analyzed from Figure 18b that when the forward speed of the machine is 1.5 km·h^{-1} and the elastic coefficient of the reset spring is a fixed horizontal value, the leakage rate between plants increases with the increase in the compression speed of the hydraulic cylinder. The main reason for this situation is that as the compression speed of the hydraulic cylinder gradually increases, the obstacle avoidance rod expands faster, the obstacle avoidance time between plants is shorter, and the leakage rate between plants increases. From the perspective of the degree of increase and decrease in the overall surface, in the interaction between the elastic coefficient of the reset spring and the compression speed of the hydraulic cylinder on the inter-plant leakage rate, the compression speed of the hydraulic cylinder has a significant effect on the inter-plant leakage rate. It can be analyzed from Figure 18c that when the elastic coefficient of the reset spring is 35 N·mm^{-1} at the intermediate level and the compression speed of the hydraulic cylinder is a fixed level value, the inter-plant leakage rate decreases with the increase in the forward speed of the random tool. From the perspective of the degree of increase and decrease in the overall surface, in the interaction between the compression speed of the hydraulic cylinder and the forward speed of the machine on the inter-plant leakage rate, the forward speed of the machine has a significant effect on the inter-plant leakage rate.

The optimal solution of the regression model was solved by using the optimization module of Design Expert 11 software. The range of test factors was as follows: the forward speed of the machine was 1.4~1.6 km·h^{-1}, the compression speed of the hydraulic cylinder was 200~260 mm·s^{-1}, the elastic coefficient of the reset spring was 25~45 N·mm^{-1}, and the minimum value of the test index was 0%. The optimal parameter combination configuration diagram is shown in Figure 19 below; that is, when the optimal solution is the tractor forward speed of 1.5 km·h^{-1}, the hydraulic cylinder compression speed is 225 mm·s^{-1}, and the elastic coefficient of the reset spring is 29 N·mm^{-1}, the inter-plant leakage rate is 7.65%.

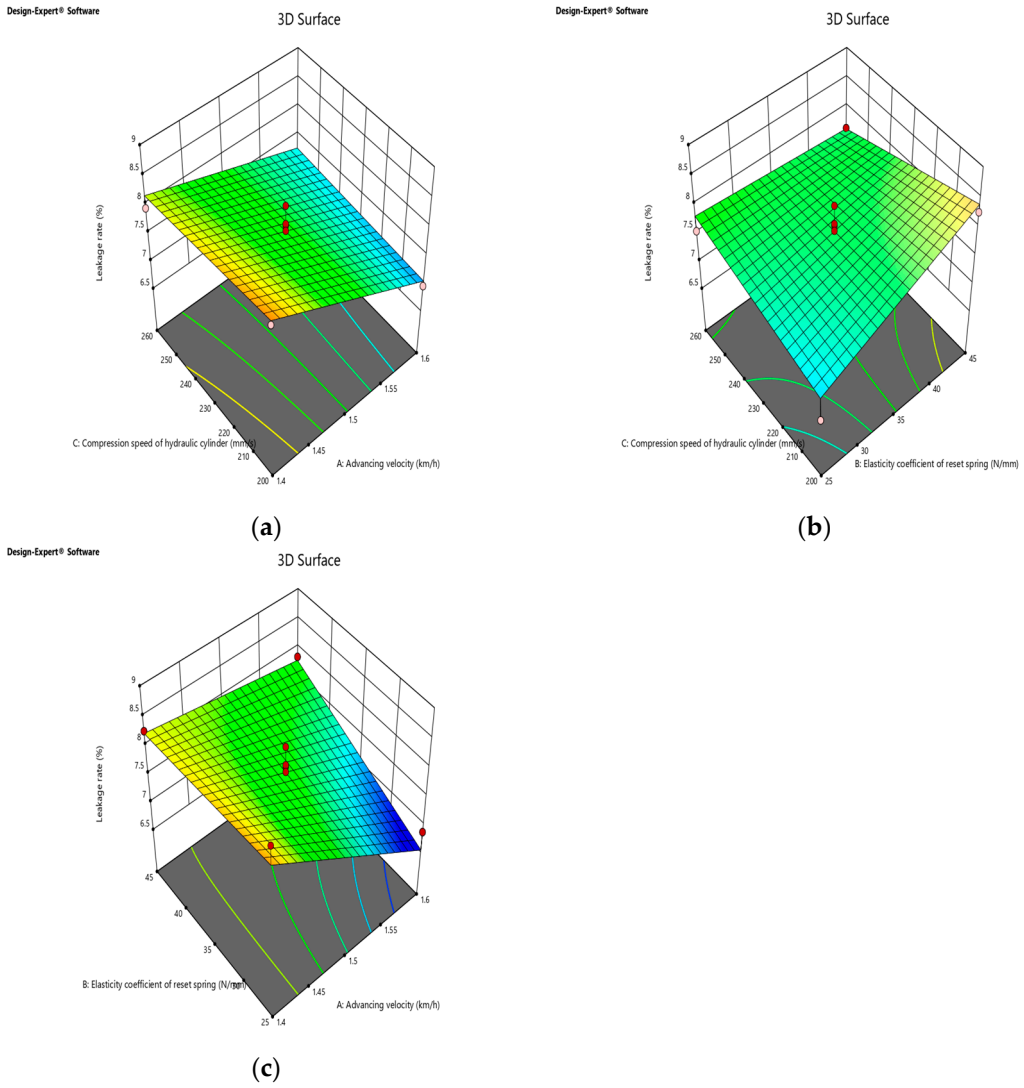

Figure 18. Effects of interaction of various factors on the rate of missing cutting between plants. (**a**) The interaction of AC on missing cutting G1 between plants. (**b**) The interaction of BC on missing cutting G1 between plants. (**c**) The interaction of AB on missing cutting G1 between plants.

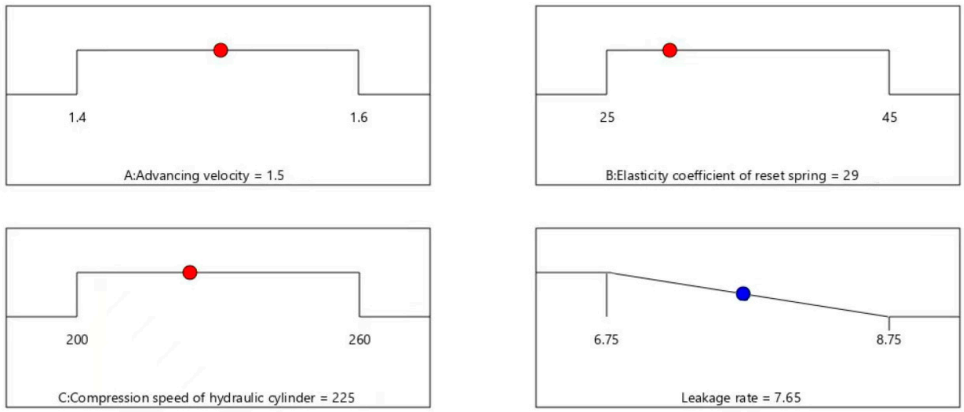

Figure 19. Optimal parameter combination configuration diagram.

5. Field Test Verification and Result Analysis

5.1. Test Purpose

The purpose of the field experiment is to detect the operation quality of the main orchard obstacle avoidance mower, verify the field operation performance of the machine, and provide a practical basis for seeking the optimal operation parameters and later optimization and improvement. Referring to the '(GB/T 5262 agricultural machinery test conditions determination method of general provisions)' [38], '(GB/T 5667 agricultural machinery production test method)' [39], '(GB 10396 Tractors, Machinery for Agriculture and Forestry, Powered Lawn and Garden Equipment. Safety Signs and Hazard Pictorials [40])' and other standards as indicators, and according to the fact that Xinjiang's main orchard generally has a 4 × 1.5 m row spacing planting pattern, this was used for field test verification.

The test contents include the leakage rate, the obstacle avoidance passing rate and the working stability of the hydraulic system of the main orchard inter-plant obstacle avoidance mower at different forward speeds. The performance evaluation index of the obstacle avoidance mower is as follows (Table 9).

Table 9. Performance evaluation index of obstacle avoidance mower.

Pilot Project	Evaluating Indicator
Leakage rate between plants (%)	<10
Obstacle avoidance pass rate (%)	100

5.2. Test Conditions and Process

A field experiment of inter-plant obstacle avoidance lawn mower was carried out in a pear orchard of the first division of the Xinjiang Production and Construction Corps, Alar City. The experimental field was a 7-year-old pear tree with a tree height of 3.5 m, a stem diameter of 20 cm, and a stem height of 65 cm and a tractor with a power calibration power of 44.1 Kw and a working speed of 1.5~3 km·h^{-1}. The test instruments include a tractor, obstacle avoidance mower, 4.5 m tape measure, 50 m tape measure, electronic stopwatch YS-801 (0~8639 s), Omron displacement sensor ZX1-LD50 A61 (range 300 mm, accuracy 0.002 mm), Edelberg HP-500 dynamometer (accuracy 0.1 N), computer, etc. The field test field and prototype are shown in Figure 20a,b below.

(**a**) (**b**)

Figure 20. (**a**) Test site. (**b**) Obstacle avoidance mower prototype.

The experimental prototype adopts a tractor with a matching power calibration power of 44.1 Kw. When the tractor's forward speed is 1.5 km·h^{-1}, the hydraulic cylinder's compression speed is 225 mm·s^{-1}, and the elastic coefficient of the reset spring is 29 N·mm^{-1}, and the working process and mowing effect of the orchard inter-plant obstacle avoidance mower are as shown in Figure 21a–c.

(**a**) (**b**) (**c**)

Figure 21. Field test verification. (**a**) Before mowing operation. (**b**) After mowing operation (between rows). (**c**) After mowing operation (between plants).

5.3. Test Results

The inter-row missed cutting rate and the obstacle avoidance pass rate of the obstacle avoidance mower are used as the evaluation index of the obstacle avoidance mower performance between the mowers. The inter-row missed cutting rate is the ratio of the actual missed cutting area to the total area of the measured area (the specific formula is shown in 3–25 above). The obstacle avoidance pass rate is the ratio of the number of fruit trees actually avoided to the number of fruit trees measured during the inter-row obstacle avoidance mowing operation of the mower. The specific formula is as follows.

$$P_1 = \frac{N_1}{N_2} \times 100\% \tag{32}$$

In the formula, P_1—the obstacle avoidance pass rate; N_1—the actual number of obstacle avoidance instances; and N_2—the total number of fruit trees in a single stroke.

The test results are shown in Tables 10 and 11 below.

Table 10. Test results of inter-plant leakage rate.

Item	Measure the Total Area /m^2	Uncut Area /m^2	Non-Tillage Area /m^2	Leakage Rate /%	The Average Leakage Rate /%
Experiment 1	3	0.39	0.16	7.75	7.64
Experiment 2	3	0.36	0.13	7.73	
Experiment 3	3	0.42	0.19	7.64	
Experiment 4	3	0.42	0.18	8.06	
Experiment 5	3	0.40	0.17	7.81	
Experiment 6	3	0.45	0.24	6.87	
Experiment 7	3	0.38	0.16	7.55	
Experiment 8	3	0.40	0.17	7.62	
Experiment 9	3	0.36	0.14	7.59	
Experiment 10	3	0.42	0.19	7.78	

Table 11. Test results of obstacle avoidance pass rate between plants.

Item	Determine the Number of Fruit Trees/Tree	Obstacle Avoidance Number/Tree	Obstacle Avoidance Pass Rate/%
Experiment 1	50	50	100
Experiment 2	55	55	100
Experiment 3	60	60	100
Experiment 4	65	65	100
Experiment 5	70	70	100
Experiment 6	75	75	100
Experiment 7	80	80	100
Experiment 8	85	85	100
Experiment 9	90	90	100
Experiment 10	95	95	100

After analyzing the test results of Tables 10 and 11 above, it can be concluded that when the forward speed of the tractor is 1.5 km·h^{-1}, the compression speed of the hydraulic cylinder is 225 mm·s^{-1}, the elastic coefficient of the reset spring is 29 N·mm^{-1}, the average leakage rate between the plants is 7.64%, and the obstacle avoidance pass rate is 100%. This shows that the working performance of the inter-plant obstacle avoidance mower is stable and the design meets the operation requirements.

6. Conclusions

(1) Aiming at the problem of the difficult removal of inter-plant weeds in Xinjiang trunk orchards, an inter-plant obstacle avoidance mower for trunk orchards was designed, which could realize inter-row and inter-plant weeds without harming the trunk. Through the further statics and kinematics simulation and theoretical analysis of the key components of the obstacle avoidance mower, the rationality of the design of the obstacle avoidance mower is further verified.

(2) The automatic obstacle avoidance device between plants was designed and studied. The structural design of the automatic obstacle avoidance device was carried out, and the working parameters of the obstacle avoidance device were determined by simplifying it into a two-dimensional model. The virtual kinematics simulation single-factor test of the designed inter-plant obstacle avoidance device was carried out by using ADAMS software. Through the reduction in and calculation of the motion trajectory of the simulation test, it was finally determined that the forward speed of the machine, the elastic coefficient of the reset spring and the compression speed of the hydraulic cylinder were the main influencing factors of the inter-plant obstacle avoidance mower.

(3) The main influencing factors determined by single-factor simulation using ADAMS and the optimal solution obtained by the quadratic regression combination test are further verified by field experiments. The results show that when the tractor forward speed is 1.5 km·h^{-1}, the hydraulic cylinder compression speed is 225 mm·s^{-1}, and the elastic coefficient of the reset spring is 29 N·mm^{-1}, the average leakage rate between the orchard plants is 7.64%, and the obstacle avoidance pass rate is 100%. The working stability is strong and meets the design requirements.

Author Contributions: Conceptualization, Y.Y., Y.H., Z.T. and H.Z.; Investigation, Y.Y., Y.H., Z.T. and H.Z.; literature search, Y.Y.; data analysis, Y.Y. and Y.H.; Writing—original draft, Y.Y., Y.H., Z.T. and H.Z.; Writing—review and editing, Y.Y., Y.H., Z.T. and H.Z.; Visualization, Y.Y. and Y.H.; Supervision, Y.H.; Project adminstration, Y.H., Z.T. and H.Z. All authors have read and agreed to the published version of the manuscript.

Funding: This research was financially supported by the Science and Technology Program of XPCC (2024BA005, 2021AA005, 2021AA0050302 and 2023GG2201).

Institutional Review Board Statement: Not applicable.

Data Availability Statement: The data presented in this study are available on request from the corresponding author.

Acknowledgments: The authors thank Yichuan He from Tarim University for his thesis supervision. The authors are grateful to the anonymous reviewers for their comments.

Conflicts of Interest: The authors declare no conflicts of interest.

References

1. Zhu, Z.; Pei, X.; Li, Y.; Yang, L.; Li, Z.; Ma, W. Investigation and Countermeasure Research on the Development Status of Mechanization of Forestry and Fruit Industry in Xinjiang. *Chin. J. Agric. Mach. Chem.* **2017**, *38*, 134–140.
2. Lao, F.; Zhang, X.; Zhang, J. Research status and analysis of orchard obstacle avoidance and weeding machine. *Hebei Agric. Mach.* **2021**, *3*, 15–16.
3. Tavakoli, H.; Mohtasebi, S.S.; Jafari, A. Physical and mechanical properties of wheat straw as influenced by moisture content. *Int. Agrophysics* **2009**, *23*, 175–181.
4. Saimbhi, V.S.; Wadhwa, D.S.; Grewal, P.S. Development of a Rotary Tiller Bladeusing Three-dimensional Computer Graphics. *Biosyst. Eng.* **2004**, *89*, 47–58. [CrossRef]
5. Ma, J. Tsui Tsui Pastoral Management Conveyor. *Mod. Agric. Mach.* **2018**, 44.
6. Ma, J. Zhushui Brand 9GZ-221 Ride Mowing Machine. *Mod. Agric. Mach.* **2017**, 45.
7. Li, D.; Zhang, L.; Gai, Z.; Wang, W. Research status of weeding technology at home and abroad. *For. Eng.* **2002**, 17–18.
8. Bai, Y.; Wang, X.; Hu, G.; Zhang, Y. Application of non-chemical methods in weed control in farmland. *J. Agric. Mach.* **2007**, *38*, 191–196.
9. Fu, X.; Mao, J.; Liu, H.; Li, J.; Gao, J.; Shen, Z.; Long, C.; Yue, J. A review of weed management techniques in organic orchards at home and abroad. *J. Weeds* **2016**, *34*, 7–11.
10. Yang, F.; Tan, C.; Fu, Z. A Three-Disc Orchard Obstacle Avoidance Mowing Device. 201710055360.5, 21 July 2017.
11. Yang, X. Current situation and development trend of mechanized weeding in orchards in organic agricultural production. *Sichuan Agric. Sci. Technol.* **2020**, 33–34.
12. Wang, D.; Wang, W.; Yi, X.; Li, P.; Liao, J.; He, Y.; Zhang, F. Present situation and development trend of orchard green manure mechanization. *J. Fruit Trees* **2021**, *38*, 421–434.
13. Zhao, Q.; Wang, H.; Yi, X.; Wang, L.; Qin, C.; Wan, C. Design and experimental analysis of orchard obstacle avoidance rotary cultivator. *Res. Agric. Mech.* **2022**, *44*, 97–100+106.
14. Chinese Academy of Agricultural Mechanization Sciences. *Handbook of Agricultural Machinery Design (II)*; China Agricultural Science and Technology Press: Beijing, China, 2007; Volume 33, pp. 53–60.
15. Wang, X.; Liao, J.; Wang, Y.; Zhao, J.; Lan, H. Discussion on the development of orchard green manure planting machinery and equipment in Xinjiang. *Henan Agric.* **2020**, 33–34.
16. Gao, H. *Agricultural Mechanization Production Science*; China Agricultural Publishing House: Beijing, China, 2022; Volume I, pp. 28–30.
17. Chen, D.; Ma, Y.; Hao, J.; Zhao, J.; Yang, X.; Li, J.; Yan, T. Design of stalk crushing knife for ear-stem corn harvester. *Agric. Mech. Res.* **2018**, *40*, 72–77.
18. Jia, H.; Jiang, X.; Guo, M.; Liu, X.; Wang, L. Design and experiment of V-L type straw crushing and returning blade. *J. Agric. Eng.* **2015**, *31*, 28–33.
19. Fu, X.; Li, M.; Lu, J.; Wang, J.; Deng, Y.; Zhang, J. Research progress of straw crushing and returning machine flail. *China Agric. Mech.* **2011**, *83–87*, 28–32.
20. Dai, Y.; Liu, Y.; Wu, Y.; Chen, X.; Liu, X. Design and test of ditching machine for facility vegetable planting. *Chin. J. Agric. Mach. Chem.* **2019**, *40*, 53–57.
21. Xiang, K. Design and Analysis of Hammer-Knife Mower. Master's Thesis, Hubei University of Technology, Wuhan, China, 2017.
22. Wang, C. Design and Experimental Study of a New Multi-Point Extrusion Walnut shell Breaking Machine. Master's Thesis, Shaanxi University of Science and Technology, Xi'an, China, 2021.
23. Huang, Z.; Liu, C. *ANSYS Workbench 14.0 Super Learning Manual*; People's Posts and Telecommunications Press: Beijing, China, 2015.
24. He, X.; Liu, J.; Wang, X.; Xu, Y.; Hu, C.; Li, Y. Design and experiment of row-to-row shoveling and laying machine for close planting cotton stalk. *J. Agric. Mach.* **2020**, *51*, 142–151.
25. Li, B. *Treasure Raft*; Agricultural Mechanics, China Agriculture Press: Beijing, China, 2003.
26. Zhao, M.; Zhang, N.; Yang, T.; Shi, Y. Design and experiment of virtual prototype of double disc mower cutter. *J. Agric. Mach.* **2014**, *45*, 101–105.

27. Li, Y.; Sun, P.; Pang, J.; Xu, L. Finite element modal analysis and test of combine harvester chassis frame. *Acta Agric. Eng. Sci.* **2013**, *29*, 38–46+301.
28. Jiang, Y.; Liao, Y.; Qin, C.; Gun, Z.; Liao, Q. 4SY-2.9 Rape Cutter Frame Vibration Analysis and Improvement. *Acta Agric. Eng.* **2017**, *33*, 53–60.
29. Su, Y. Optimization Analysis and Trial Production Verification of Rotary Tillage Device in Northeast China. Master's Thesis, Harbin University of Technology, Harbin, China, 2019.
30. Li, Z. *Introduction and Example of ADAMS*; National Defense Industry Press: Beijing, China, 2006; pp. 171–176.
31. Li, C.; Zeng, W.; Xu, D.; Yang, Y. Kinematics Simulation of the Cam Mechanism of the Zipper Machine Based on ADAMS. *IOP Conf. Ser. Mater. Sci. Eng.* **2019**, *612*, 032146. [CrossRef]
32. Hang, A.; Liao, P.; Li, W.; Liu, Y. Analysis of cotton stubble waste film collection and baling machine based on ADAMS. *Agric. Mech. Res.* **2018**, *40*, 22–27.
33. Zhu, Z. Design and Experimental Study on Automatic obstacle avoidance device for inter-plant weeding in orchard. Master's Thesis, Shihezi University, Shihezi, China, 2020.
34. Du, Y.; Mao, E.; Song, Z.; Zhu, Z.; Gao, J. Simulation of corn plant harvest process based on ADAMS. *Agric. Mach. J.* **2012**, *43* (Suppl. S1), 106–111.
35. Wang, Y.; Zhang, D.; Yang, L.; Cui, T.; Li, Y.; Liu, Y. Design and experiment of hydraulic excitation source self-excited vibration subsoiler. *Acta Agric. Eng. Sci.* **2018**, *34*, 40–48.
36. Zhao, S.; Tan, H.; Wang, J.; Yang, C.; Yang, Y. Design and experiment of multifunctional integrated seeding furrow opener. *Acta Agric. Eng.* **2018**, *34*, 58–67.
37. Yao, W.; Zhao, D.; Miao, H.; Cui, P.; Wei, M.; Diao, P. Design and experiment of oblique anti-blocking device for shallow rotary stubble cleaning of no-till planter. *Agric. Mach. J.* **2022**, *53*, 42–52.
38. *GB/T 5262*; Measuring Methods for Agricultural Machinery Testing Conditions. General rules; National Standardization Technical Committee of Agricultural Machinery: Beijing, China, 2009.
39. *GB/T 5667*; Productive Testing Methods for Agricultural Machinery. The Standardization Administration of the People's Republic of China: Beijing, China, 2009.
40. *GB 10396*; Tractors, Machinery for Agriculture and Forestry, Powered Lawn and Garden Equipment. Safety Signs and Hazard Pictorials. General Principles; National Agricultural Machinery Standardization Technical Committee: Beijing, China, 2006.

Disclaimer/Publisher's Note: The statements, opinions and data contained in all publications are solely those of the individual author(s) and contributor(s) and not of MDPI and/or the editor(s). MDPI and/or the editor(s) disclaim responsibility for any injury to people or property resulting from any ideas, methods, instructions or products referred to in the content.